Modeling water absorption in cement-based composites with SAP additions

Romero Rodriguez, Claudia; Chaves Figueiredo, Stefan; Schlangen, Erik; Snoeck, D

Publication date
2018

Document Version
Final published version

Published in
Computational Modelling of Concrete Structures

Citation (APA)
Romero Rodriguez, C., Chaves Figueiredo, S., Schlangen, E., & Snoeck, D. (2018). Modeling water absorption in cement-based composites with SAP additions. In G. Meschke, B. Pichler, & J. G. Rots (Eds.), *Computational Modelling of Concrete Structures: Proceedings of the Conference on Computational Modelling of Concrete and Concrete Structures* (pp. 295-304). CRC Press.

Important note
To cite this publication, please use the final published version (if applicable).
Please check the document version above.

MODELING WATER ABSORPTION IN CEMENT-BASED COMPOSITES WITH SAP ADDITIONS

C. Romero Rodríguez, S. Chaves Figueiredo & E. Schlangen
Department of Structures
Microlab, Delft University of Technology,Delft, the Netherlands

D. Snoeck
Department of Structural Engineering and Architecture
Magnel Laboratory for Concrete Research, Ghent University, Ghent, Belgium

ABSTRACT: The ability of Superabsorbent Polymers (SAP) to block water flow through cracks in cement-based materials has become an attractive feature of these admixtures. The diminution of flow rates in such composites are attributed to the capacity of the SAPs to absorb water and swell in the crack, but little work has been done to indicate one or the other cause. On the other hand, the SAPs present in the bulk matrix might act as distributed sinks through which water is absorbed (water that otherwise would have continued its path into the matrix). In this paper a preliminary effort is made to numerically model the effect of SAPs on the water absorption by mortar. A lattice-type model is proposed to predict both the bulk water absorption and the resulting penetration depth of water into the cementitious matrix. The results of the simulations point out the mechanisms of water absorption in mortar containing SAPs.

1 INTRODUCTION

Cement-based materials are largely used for construction purposes due to their relatively high compressive strength and low costs. Nevertheless, the porous structure of this composite allows the ingress of harmful species into the material. Eventually, these species degrade the matrix or the reinforcement leading to irreversible damage in the material if left without intervention. Such consequences can be further aggravated when cracks form during the service life of concrete elements, providing preferential paths through which the external deleterious agents penetrate into the material. In all cases, water is necessary for the transport of the external substances (chlorides, sulfates, CO_2, etc.).

In order to block water penetration into the matrix when cracks are present, Superabsorbent Polymers (SAP) have been proposed in literature to potentially obtain a self-sealing effect in the crack (Kim & Schlangen 2010). SAP are polyelectrolite gels which can absorb and retain large quatities of water with respect to their own weight. The swelling of these particles is driven towards the achievment chemical and physical equilibrium of the polymeric chains when in contact with a solution. The individual particle swells until the sum of all acting pressures upon it is zero (Vervoort 2006). In a polyelectrolite gel the main pro-swelling pressures are of osmotic nature, related to the repulsive Coulomb forces between charged chains, etc.. On the other hand, the counteracting pressures might be of an elastic nature within the gel, due to external forces, etc..

Many experimental studies have been performed regarding hydrogel formation inside cracks in cementitious materials. Permeation tests performed by Hong and Choi (2017) on SAP containing mortars showed reductions of 75% and 63% of the water flow rates for crack widths of 250 and 350 μm, respectively, on mortars with 1% of SAPs by weight of cement. In a work of Snoeck et al. (2012) Neutron Imaging was performed during water absorption tests in mortars with SAPs of different types and in various dosages. The results presented in the study show reduced depths of penetration of the wetting front in mortars with SAPs with respect to the plain reference mortars, in both horizontal and vertical directions. Such mixtures had no additional water. Snoeck et al. (2015) also demonstrated the reduction in poros-

ity of the same cementitious matrices containing SAPs due to their internal curing effect. Despite all evidence regarding the reduced permeability and capillary absorption provided by these admixtures in cracked cement-based materials, the experimental methods used do not clarify the mechanisms of crack self-sealing by SAPs. Reduced capillary absorption in the densified matrix and consequent flow instabilities in the crack or swelling and absorption in the SAPs might also be the causes of such an effect. It is interesting to investigate the influence of each mechanism on the sealing ability to optimize the material through numerical models.

In this work, a numerical model is presented to predict the capillary absorption of mortar with SAP admixtures. As a basis for modeling the overall physical problem, the well-established Richards equation is used to describe the capillary absorption in the bulk matrix, in combination with the exponential law for the hydraulic diffusivity in cement-based materials. In parallel, a diffusive-type law for the water uptake of SAPs is implemented as sink term in the diffusion equation. A lattice approach is used for the discretization of the domain. Heterogeneity of transport properties is explicitly modeled with this method, not only through the discrete distinction between SAPs and mortar but also through the use of an irregular lattice mesh for the simulations. The model was validated through available experimental data, first of the capillary absorption in plain mortar and secondly of mortar containing SAPs. On one hand, input parameters for the modeling of water absorption in mortar were also available for the different validating data sets. On the other hand the parameters needed for the description of water uptake by SAPs were missing, therefore a loose fitting procedure was implemented for this purpose.

The focus of this paper is on the qualitative validation of the presented model. The obtained results enable the use of the diffusive-type law of water absorption by SAPs inside the matrix and its use as a starting point for modeling the crack self-sealing by SAPs, as long as the necessary input parameters are available. Conclusions could be drawn for the mechanisms of water absorption in mortar with SAP admixtures.

2 FORMULATION OF THE PHYSICAL PROBLEM

In this section a brief derivation is offered of the governing equations for the studied problem. First, we introduce the simplified equation for the unsaturated flow in porous media and the empirical laws used for the derivation of its parameters in porous building materials. In the second part, the equation for the swelling kinetics of a single spherical SAP particle is reported.

2.1 *Theory of unsaturated water movement in sound cement-based composites driven by capillary absorption*

Starting from the two mass balance equations for air and water and Darcy's extended law for the flow velocity, one can arrive at the two-phase formulation of immiscible flow in a homogeneous porous media. The complicated resulting system can be simplified if certain conditions are met, leading to the Richards equation for the unsaturated water flow in porous media (Szymkiewicz 2013). The conditions for the validity of Richards equation in cementitious materials have been reported in (Szymkiewicz 2013). In sum, isothermal conditions around 20 °C ensure the correctness of the assumption of uncoupling the water and air transport if they are assumed to be continuous throughout the pore space. Below, the potential form of such equation is reported:

$$C(\theta)\frac{\partial \phi}{\partial t} = \nabla(K(\theta)\cdot\nabla\phi) + S(\theta,t) \tag{1}$$

Where ϕ is the hydraulic potential $[L]$, sum of the water head (h) , capillary (ψ) and gravitational (z) potentials; $S(\theta,t)$ contains sinks or sources; $K(\theta)$ $[LT^{-1}]$ is the unsaturated permeability function and $C(\theta)$ $[L^{-1}]$ is the so-called capacity or storage coefficient defined as:

$$C(\theta) = \frac{d\Theta}{d\phi} = (\Theta_s - \Theta_i)\frac{d\theta}{d\phi} \tag{2}$$

Where $(\Theta_s - \Theta_i)$ represents the difference between volumetric water content at saturation and at the start, which in a way represents the porosity accessible to water of the material $[-]$ and θ is the water saturation $[-]$.

If gravitational and waterhead potentials are considered to be negligible with respect to the capillary potential and the hydraulic diffusivity, $D(\theta)$ $[L^2T^{-1}]$, is defined as:

$$D(\theta) = \frac{K(\theta)}{C(\theta)}\nabla\phi \tag{3}$$

Equation 1 can be transformed into:

$$\frac{\partial \theta}{\partial t} = \nabla(D(\theta)\cdot\nabla\theta) + s(\theta,t) \tag{4}$$

The advantage of the PDE formulated as in equation 4 lies on the fact that $D(\theta)$ can be approximated as (Hall & Hoff 2009):

$$D(\theta) = D_0 e^{n\theta} \tag{5}$$

Where n has been proven to lay between 6-8, varying little among materials. In this work, n is assumed to have value 6, unless otherwise specified. D_0 can be estimated from sorptivity experiments with good results, as proposed by Lockington et al. (1999):

$$D_0 = \frac{n^2 S^2}{(\Theta_s - \Theta_i)^2 [e^n(2n-1) - n + 1]} \tag{6}$$

And the Sorptivity S being defined as the slope of the best-fit line of the curve Cumulative water penetration vs. $[T^{1/2}]$.

The system of equations describing the water absorption in unsaturated cement-based materials results then in the parallel implementation of Equations 4 and 5.

The problem of water absorption in the studied material, to be implemented in 3D, has the following Boundary and Initial Conditions:

$$\begin{aligned} &\theta = 1 && \text{on } \Gamma_1 \\ &\frac{\partial \theta}{\partial n} = 0 && \text{on } \Gamma_2 \\ &\theta(t=0) = \theta_{initial} && \text{in } \Omega \end{aligned} \tag{7}$$

2.2 *SAP swelling kinetics*

Esteves (2011) and Sweijen et al. (2017) described the swelling kinetics of spherical SAP particles as a diffusion-governed process depending only on their diameter, provided a certain ionic composition of the solution and a certain type of SAP. Esteves (2011) validated such a model by monitoring the change in time of SAP's diameters. The differently sized particles were immersed in a micro-bath and observed under an optical microscope. In particular, Esteves assumed the hydrostatic pressure of the microbath negligible to the swelling pressure and a constant particle density to calculate the water uptake.

The swelling law (in Equation 8) was presented by the author in terms of the swelling capacity at equilibrium, Q_{max}, and at a given time t, Q.

$$\frac{dQ}{dt} = k(Q_{max} - Q) \tag{8}$$

The constant rate k, dependent on the particle diameter ϕ_{SAP} , is shown in Equation 9.

$$k = r_1 \phi_{SAP}^{-r_2} \tag{9}$$

The constants r_1 $[L^{-r_2}/T]$ and r_2 $[-]$ depend on the swelling medium and the SAP type under consideration. Their values should be fitted from experiments carried out like in the work mentioned above while monitoring as well the amount of absorbed water.

Since for the problem of resolving water absorption in mortar with SAP particles the interest is on the amount of absorbed water in time by the SAP rather than their change in dimensions, the authors hypothesized an extension of the swelling kinetics law to the volume of absorbed water instead. Herein, we assumed that the volume of the particle at equilibrium, $V_{SAP_m,max}$, is as follows:

$$V_{SAP_m,max} = \frac{Ab_{sol}\rho_{dry}}{\rho_{sol}} V_{SAP,dry} \tag{10}$$

Where Ab_{sol} is the absorption capacity of the SAP in the solution, ρ_{dry} and ρ_{sol} are the densities of the dry SAP and the solution, respectively and $V_{SAP,dry}$ is the volume of the dry SAP particle.

3 NUMERICAL AND EXPERIMENTAL METHODS

In this section we briefly summarize the numerical methods used to model the problem of water absorption in unsaturated mortar. In addition, a brief explanation of the simulated experiments is offered, although no experiments were specifically carried out purposely for the validation of the model presented here.

3.1 *Mesoscale Lattice Network Model*

Lattice network models have been successfully implemented to simulate mechanical behavior of cementitious materials (Schlangen & van Mier 1992). Lately, they have also found applications in mass and ionic transport in such materials (i.e. moisture, water, chlorides) (Šavija, Pacheco, & Schlangen 2013; Wang, Bao, & Ueda 2016). These types of models consist in an assembly of discrete two-nodes elements (lattice beams) that represents a continuum. For the modeling of transport, the lattice approach treats the transport as occurring along the beam elements in the lattice mesh. Other studies (Grassl & Bolander 2016) defend the implementation of the transport in cracked materials occurring along the facets of the Voronoi poligons (in 2D). Herein, the transport is regarded as along the lattice beams.

For the discretization of the domain, the nodes are placed pseudo-randomly inside each cubic cell of a quadrangular grid. The specified sub-cell dimension with respect to the cubic cell determines the randomness of the set of nodes. For the

mesh generation, we choose a randomness coefficient of 0.5. Subsequently, a Voronoi tessellation is performed with respect to the previously placed nodes in the domain. Nodes belonging to adjacent Voronoi cells are joined by lattice beams as schematized in Figure 1.

The advantage of lattice-type models for unsaturated flow in cement-based materials is, among others, the explicit implementation of heterogeneities in the material. Sound cement paste, cracked domain, aggregates, SAP particles, Interfacial Transport Zone (ITZ) and other interfaces are assigned different lattice phases and corresponding transport properties. A schematic of such implementation for concrete in 2D is shown in Figure 2.

In this work, only mortar, regarded as one phase, and SAP phases are explicitly implemented in the mesh of the SAP mortar, as well as their interface. Anm model (Qian, Garboczi, Ye, & Schlangen 2016) was used for parking irregular-shaped SAPs into a 5mm cube with fully periodic boundaries. The cube was later used as primary cell in the creation of a specimen with larger dimensions. Such a procedure reduced drastically the computational time. The simulated SAP particles had the dimensions of the macropores left by the desorption of the SAP.

The binary tomography was used to discriminate between mortar and SAP phases in the mesh by overlapping both grids: nodes in the lattice mesh inside a cell belonging to a certain phase are tagged with such a phase. Similarly, beam elements with nodes belonging to the same phase were tagged as such, while elements bridging both faces were distinguished as interface elements. Although, since the transport properties of the interface zone between SAPs and the surrounding mortar were unknown, similar properties to the mortar were assigned with good approximation since the

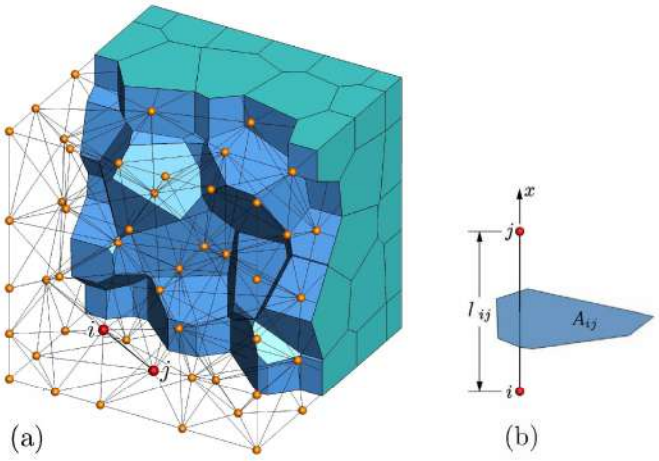

Figure 1: Schematics of spatial discretization with Voronoi Tessellation (Pan, Prado, Porras, Hafez, & Bolander 2017).

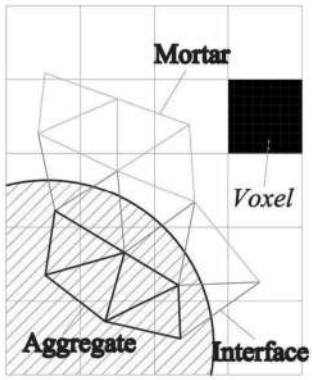

Figure 2: Heterogeneity implementation in a 2D lattice mesh (Savija 2014).

SAPs provide internal curing.

3.1.1 *Numerical implementation*

If Equation 4 is discretized by using Galerkin method, in the context of lattice model its weak formulation in matrix form results:

$$M\frac{\partial\theta}{\partial t} + K\theta = F \tag{11}$$

Where the M and K are the mass and diffusivity matrices, respectively. F is the forcing vector, in which the Neumann-type boundary conditions and any sink/source terms are dumped. The elemental matrices and vectors described above are reported in Equations 12, 13 and 14 for the ij element in its local reference system:

$$m_{ij} = \frac{A_{ij}l_{ij}}{6\omega}\begin{bmatrix}2 & 1\\ 1 & 2\end{bmatrix} \tag{12}$$

$$k_{ij} = \frac{D_{ij}(\theta)A_{ij}}{l_{ij}}\begin{bmatrix}1 & -1\\ -1 & 1\end{bmatrix} \tag{13}$$

$$f_{ij} = \begin{bmatrix}f_i\\ f_j\end{bmatrix} \tag{14}$$

A_{ij} and l_{ij} are the elemental area and length. While ω is a correction parameter for the volume of the single element. It has been proven that, being ω the ratio between the sum of all elements volume in the mesh and the volume enclosed by the mesh boundaries, its value results 3 for three-dimensional meshes (Asahina et al. 2014).

Crank–Nicholson scheme is used for the time discretization.

$$(M + \frac{1}{2}\Delta t K^{n-1})\theta^n = (M - \frac{1}{2}\Delta t K^{n-1})\theta^{n-1} + \Delta t f$$

(15)

An iterative algorithm is avoided by calculating θ of the current time step (n) using the K matrix calculated at the previous step $(n-1)$. Although an error is introduced in the solution of the system, it is small for appropriately short time steps. Such a procedure was used by Luković et al. (2016) to model the drying of cementitious materials with good results .

3.1.2 *SAPs water absorption: sink term or high transport properties?*

On one hand, SAPs are regarded as sinks for the current physical problem. On the other hand, from the moment that SAPs are considered as another phase in the modeled mortar, transport properties need to be assigned to the the beam elements corresponding to the SAP domain. Roughly saying, the following statement applies: water that does not get in cannot be absorbed. The hydraulic diffusivity of SAP beam elements for the current time step n was then approximated as:

$$D^n_{ij,SAP_m} = \frac{k_{SAP_m}(V_{m,max} - V^{n-1}_m)}{l_{ij}} \tag{16}$$

In a similar fashion the sink term was implemented as follows. The volume of water absorbed by the node $i-$ at the current time step was estimated as:

$$f^n_{i,SAP_m} = \frac{k_{SAP_m}(V_{m,max} - V^{n-1}_m)}{\sum_{i\in m} V_{cell,i}} V_{cell,i} \tag{17}$$

Where $V_{cell,i}$ is the volume of the Voronoi cell associated to node $i-$.

3.2 *Capillary absorption experiments and input parameters*

Different procedures are used in the laboratory for the measurement of the sorptivity of cementitious materials (ASTM 2008; CEN 2002). Basically, the methods differ on the preconditioning of the samples prior to the test, aimed to achieve an even moisture distribution inside the sample with prescribed dimensions.

In any case, the samples lateral surface is waterproofed and the top surface is loosely covered to avoid the buildup of pressure that may hinder the unidirectional flow of water in the sample while preventing moisture exchange at that boundary. The samples are placed on narrow supports inside a container and the water level is kept constant at 2-3 mm from the bottom of the sample. The mass increase of the sample is monitored over time throughout the test, more frequently during the first hours as the bulk of the water absorption occurs in this interval of time. The results are presented as a plot of the weight per unit of area exposed to saturation against the square root of time. S is determined as the slope of the best fit line in the first 4-6 hours since afterwards the gravitational forces start balancing the capillary forces, etc. resulting in a flattened curve. A schematic of the test is shown in Figure 3.

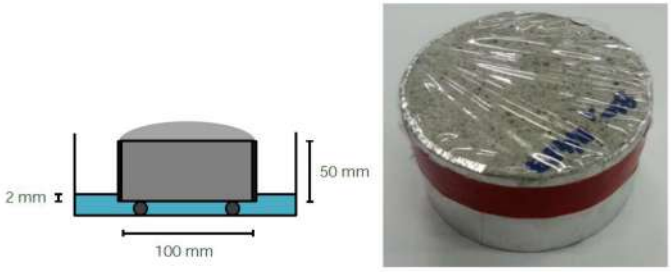

Figure 3: Capillary absorption test setup (Snoeck 2015).

For the imposition of the initial conditions, the internal moisture content must be known. Also the sorptivity S and the porosity of the material accessible to water are needed for the calculation of D_0. The latter must be known also for the quantification of the absorbed water.

Regarding the SAPs, the input parameters needed for the model are their size distributions at the dry state and at the swollen state during mixing, their absorption during mixing and their dry density. In addition, ideally the constants describing the swelling kinetics of used SAPs should be obtained from the experiment described in (Esteves 2011).

4 MODEL VALIDATION

In this section, the numerical model described in the previous section was validated with available experimental data. The validating procedure consisted of two parts. In the first part, simulations of capillary absorption in sound plain mortars were compared to available experimental data. In the second part, simulations on the coupling of capillary absorption in porous mortar matrix and water absorption by SAPs embedded in it were compared to the experimental results of sorptivity tests performed on SAP mortar.

4.1 *Mesh sensitivity analysis*

For the sake of optimizing computing speed, the influence of the cell size on the goodness of the simulation results was investigated. Voxel sizes of 0.25, 0.5 and 1.0 mm were used to discretize a mortar prism 20 mm high and square base with 10 mm side. Consequently, simulations were carried out on

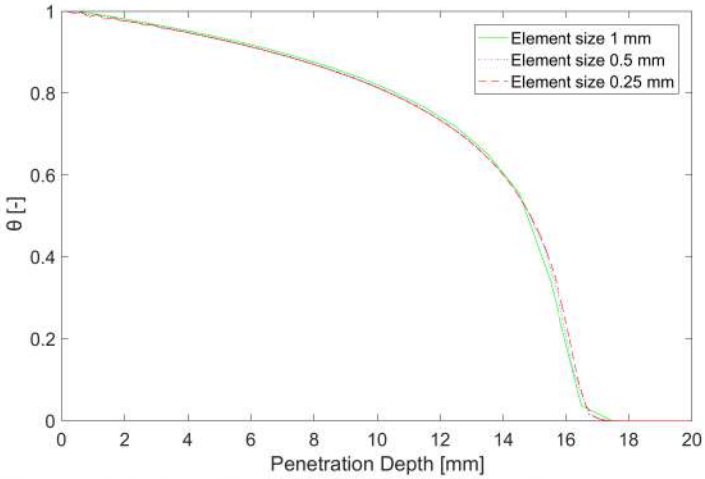

Figure 4: Saturation profiles along the direction of flow for different mesh sizes.

meshes with 128000, 16000 and 2000 nodes, respectively. The resulting amount of beam elements was 942874, 111653 and 12480, respectively. D_0 was set as 0.0231 mm^2/min and the initial saturation null. The simulations were carried out with a time step of $\Delta t = 0.25$ min and total time $t = 60$ min.

The results in Figure 4 show little differences between the different meshes for the orders of magnitude of the given hydraulic diffusivity and mesh sizes. As follows, the simulations will be carried out with element lengths of approximately 1 mm, with exception of the simulations on SAP mortar, where SAPs dimensions require a refinement of the mesh.

4.2 *Capillary absorption simulations in Plain Mortar*

The numerical model regarding only capillary absorption of water was applied to simulate two different experiments, the results of which are available in literature, as well as the necessary input parameters.

Experimental data obtained from the measurement of moisture profiles in initially dry mortar with Nuclear Magnetic Resonance (NMR) were performed by Hall (1989). The mortar specimen had dimensions of 235 x 33 x 33 mm. In the experiment, one of the bases of the prism was brought into contact with a water reservoir and the water content distribution was measured at a series of elapsed times. The porosity accessible to water was estimated as 0.27, the sorptivity, measured in the experiments as well, was 2.57 $mm/min^{1/2}$ and the diffusivity from it calculated was 0.736 mm^2/min. Figure 5 shows the simulation results versus the data points provided by the author. Overall, the simulation results matched very well with the experimental ones, hence the model provides a good prediction of the water spatial distribution and content over time.

In yet a similar experiment, Van Belleghem et al.

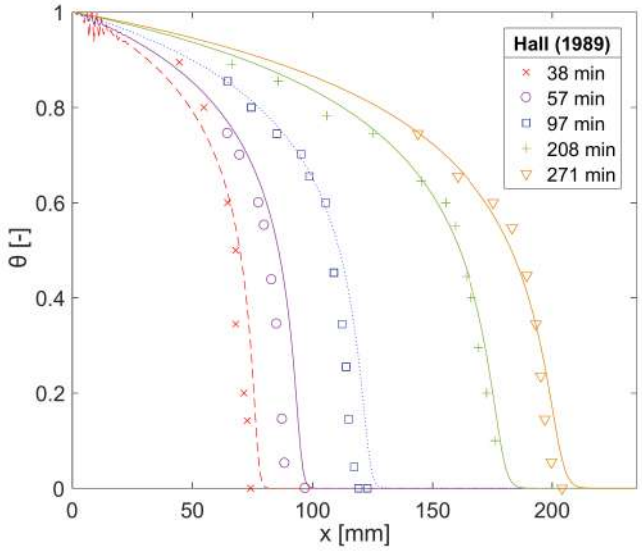

Figure 5: Comparison of saturation profiles between simulated (continuous lines) and NMR profiles (data points) after 38, 57, 97, 208 and 271 min of water absorption.

(2016) used X-ray radiographs to monitor the advancement of the wetting front and the water content distribution in unsaturated mortar. The study also presented the results of the sorptivity test in terms of global water uptake by the mortar over a time interval of 100 h. The authors obtained the necessary transport properties from the latter experiment and numerical fitting as $D_0 = 0.006$ mm^2/min and $n = 6.4$. Porosity of 0.1977 and initial saturation of 0.25 were determined experimentally prior to the absorption test. The first four hours of the sorptivity experiment were simulated with such input data by using the lattice model proposed herein. Figure 6 shows the comparison between the transient water content distributions obtained through X-ray measurements and the simulated counterpart. It can be noted how both results are in good agreement with exception of the local effects that in the model are not explicitly taken into consideration.

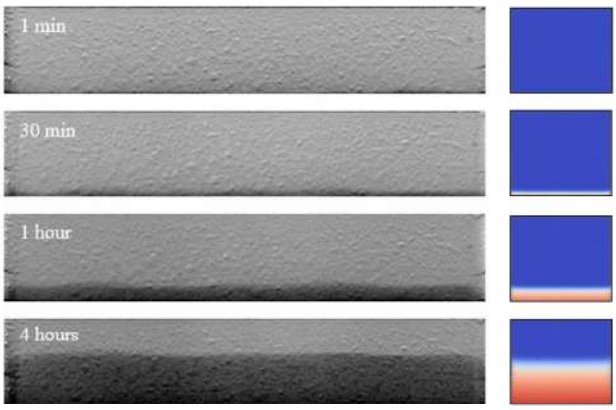

Figure 6: Comparison between X-ray radiographs (Van Belleghem et al. 2016)(left) and simulated water absorption (right) at 1 min, 30 min, 1 h and 4 h.

Table 1: Input parameters for the mortar phase used in the simulation of capillary absorption in Plain and SAP mortars.

	Transport properties		Physical parameters	
Mixture	$S[\frac{mm}{min^{1/2}}]$	$D_0[\frac{mm^2}{min}]$	Porosity	$\theta_{initial}$
R0.50	0.0341	0.0016	0.077	0.16
R0.46	0.0186	0.00097	0.068	0.18
B1.0	0.0186	0.001	0.064	0.19

4.3 *Plain Mortar vs. SAP mortar: water absorption*

Sorptivity test results are reported in (Snoeck 2015) for SAP mortars and their reference mixtures with the same effective water to cement ratios. The author also provided information on the apparent porosity and initial water content of the specimens. These input parameters are summarized in Table 1. In this paper, only SAP B series was used for the qualitative validation of the model, namely B1.0, with 1% of SAPs by weight of cement, and the plain references R0.46 and R0.50, with the same effective water-to-cement ratio and with the same total water-to-cement ratio, respectively.

In a previous work (Snoeck et al. 2015), the data attaining to the swelling properties of SAP B, used in the above experiments, were determined experimentally. SAP B were cross-linked potassium salt polyacrilates with diameters in the range of $477 \pm 53\ \mu m$ at the dry state. The absorption capacity during mixing was determined experimentally by the author by means of vapor sorption experiments. The absorption capacity during mixing was also used as the maximum nominal absorption capacity during the capillary absorption test. The latter choice is motivated by the fact that each SAP particle is constrained by the boundaries of the macropore containing it. The absorption capacity was then set as $8.9\ g/g_{SAP}$.

For the sake of obtaining a qualitative validation, two prisms with dimensions 20 x 5 x 5 mm were simulated for the studied mixtures. For the calculations of maximum volumes of water absorbed by the SAPs, the particles were assigned diameters of the equivalent spheres with same surface area as the irregular SAP particles simulated with Anm.

The mortar phase in the SAP mortar was assigned transport properties based on the sorptivities of the reference plain mortars with similar porosity. The latter simplification is accurate enough since all the mixtures were tested under the same conditions and the initial moisture content was very similar among the different mixtures (Hall 1989).

The simulated and measured absorption of water per unit area normalized to the density of water

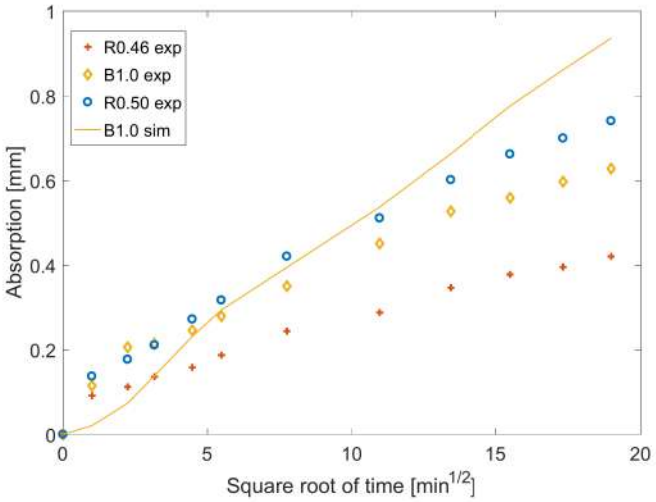

Figure 7: Absorption of water per unit area of Plain and SAP mortars.

for the different mixtures are shown in Figure 7 for different elapsed times in an interval of 6h from the moment of first contact with water. The constant of the of swelling kinetics law were loosely fitted as $r_1 = 2000\ \frac{\mu m^{1.267}}{min}$ and $r_2 = -1.267$ and the motivation is explained further in this section.

With regards to the mortars with embedded SAPs, one can observe in the graph that there is a deficiency in the water absorption of the simulated specimens in the first 20 minutes of the time-dependent analysis with respect to the measured ones. The cause for this abnormality might be the lack of SAPs at the boundary in contact with water and the low sorptivity of the matrix which leads to a delayed first contact of the lower SAPs with the upcoming water. Nevertheless, the model is able to capture similar slopes as in the experimental data for the studied time interval. After the first SAPs start absorbing water, a steeper increase on the water absorption is observed at the beginning with respect to the reference due to the uptake of water by the SAPs reached by the wetting front. As the SAPs left behind by the water front get saturated, their rate in water absorption decreases while the new ones, being reached by the water rising in the pores, start absorbing faster, overcompensating for the latter decrements. After the first 3 hours of the simulation, the deficiency in water absorption in the simulation is switched and the simulated results grow faster than those of the experimental data. The authors believe that the porosity of the mortar matrix has been overestimated, due to the high density of SAP macropores.

In order to validate this hypothesis the estimated water absorption of the SAPs was calculated from the simulations and compared to the absorption of SAPs that would has been obtained from the experimental data for different values of the sorptivity of the matrix. In Figure 9 the latter is reported for the best fit found, being the corre-

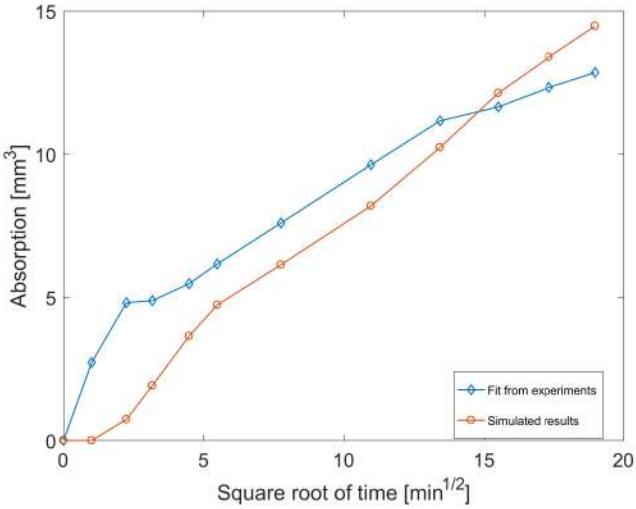

Figure 8: Amount of water absorbed by SAPs overtime in the simulations and fitted from the experimental results for $S = 0.006\ mm/min^{1/2}$.

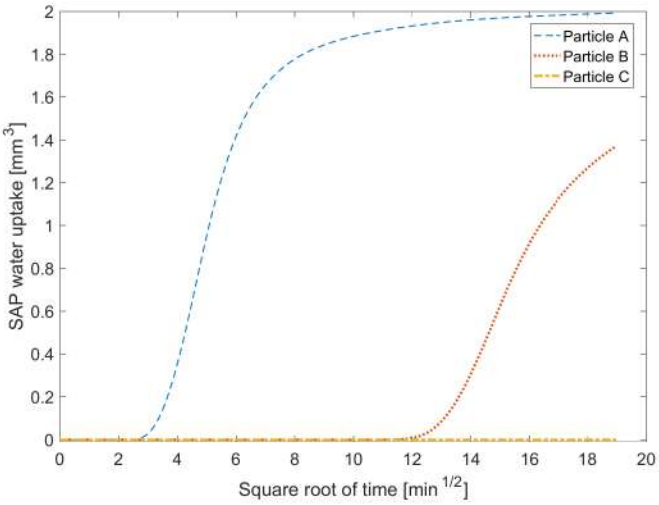

Figure 9: Absorption of water by individual SAPs at different heights along the sample.

sponding sorptivity, $0.006\ mm/min^{1/2}$, three times smaller than the one estimated from the measured apparent porosity. Although the overall behavior of the absorption curve agrees with the square root law for the sorptivity found in the experiments, the fitted rates in the SAP swelling kinetics law are by no means correct due to the shift in water absorption of the SAP and the uncertainty on the correctness of the chosen value of the sorptivity.

Evidence of the role of SAP water absorption on the curve behavior can be observed in Figure 8. The Absorbed water vs. the square root of time is reported for three identical particles placed at different heights in the simulated sample. Particle A is positioned at 1.675 mm height from the boundary subjected to contact with water, B is at 6.775 mm and C at 11.65 mm. At time $t = 180min$ the wetting front is located at 7.5 mm circa from the bottom of the sample and the surroundings of the particles have saturation of 0.94, 0.39 and 0.19 (equilibrium), respectively.

5 ADDITIONAL CONSIDERATIONS

Since the mortars studied in the previous section present low levels of porosity, the rise of the wetting front was very slow as well as the absorption of the SAPs. In this section, a hypothetical case study is presented on the comparison of two mortars with the same porosity, one containing 1% (by weight of cement) of a hypothetical SAP with fast rates of water uptake and one plain mortar. The objective is to obtain information regarding the entity of the penetration depths at different elapsed times during absorption for the sake of comparison.

Same geometry of prisms as in Section 4.3 was used. The hydraulic diffusivity, the porosity and the initial water content of the mortar phase were the same for both materials: $0.012mm^2/min$, 0.15 and 0.19, respectively. For the SAPs, same properties as in the previous section were assigned while the rates are now $r_1 = 2.76x10^5\ \frac{\mu m^{1.267}}{min}$ and $r_2 = -1.267$.

Figure 10 shows the results of the simulations for Plain (a,c,e) and SAP (b,d,f) mortars at different times during the water absorption simulations (10, 60 and 120 min).

During the first 10 min, both materials behave similarly. As seen in Section 4.3, when water encounters the first SAPs, these start absorbing water with a fast rate but since they don't occupy entirely the volume of the macropore, water can also flow out of the cavity, therefore behaving like semi-permeable inclusions. As the SAPs get saturated, they stop absorbing water and act as impermeable inclusions (Asahina, Kim, Li, & Bolander 2014), similar to the effect of aggregates on fluid transport in concrete. At this stage, water has to turn around the macropore, elongating its path upwards.

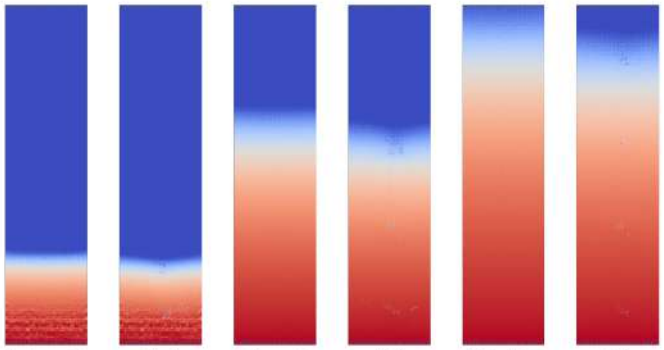

Figure 10: Penetration depths at different elapsed times during sorptivity simulations of plain (a,c,e) and SAP (b,d,f) mortars.

6 CONCLUSIONS

In this work, an attempt has been made to model the water absorption in unsaturated mortars with and without SAPs. First, the authors derived the mathematical and numerical formulations and motivated the assumptions made. In the second part, a validating procedure was performed by using available experimental data. Last, the model was used to formulate conclusions regarding the mechanism of water absorption of mortars containing SAPs.

In particular:

1. The numerical model regarding the capillary absorption of water by plain sound mortars agreed very well with the experimental results published by different authors. Although it was not implemented in the plain mortar simulations, the model can account for the presence of heterogeneity in the material, i.e. porous reinforcement interface, aggregates, ITZ, etc. as seen for the SAP mortars where SAP particles are another phase in the mesh.

2. A diffusion-controlled law for the SAPs swelling kinetics was extended to the SAPs water absorption during sorptivity simulations in mortars. Although the absorption vs. square root of time of simulated and experimental data did not fit perfectly, the overall behavior of the curve was captured in the simulations, validating the appropriateness of the law for the description of the water uptake of SAPs embedded in a cementitious matrix.

3. The model is very sensitive to the value used for the sorptivity. The results suggest that the porosity of the SAP mortar was overestimated and therefore the assumption of interpolated sorptivity of the mortar phase with respect to the porosity of the reference mixtures failed. In particular, the sorptivity was re-estimated to be one third of the one used in the simulations.

4. Finally, some considerations were made regarding the role of SAP particles in the absorption of water in mortar. At first, the particles act as semi-permeable inclusions that attract the flow of water towards it due to the higher hydraulic diffusivity. When the particle has uptaken a certain amount of water, the diffusivity of the phase drastically decrease and the particle starts behaving as an impermeable particle. The simulation results suggest that although the material under study uptakes more water globally with respect to its plain counterpart, it does reduce relatively the water rise. The latter conclusion should be explicitly validated.

7 ACKNOWLEDGEMENTS

This research is supported by a grant (17SCIP-B103706-03) from Construction Technology Research Program funded by Ministry of Land, Infrastructure and Transport of Korean Government. The financial support of this institution is gratefully acknowledged. Also, the authors wish to acknowledge Dr. Branko Šavija and Dr. Zhiwei Qian for their highly appreciated help.

REFERENCES

Asahina, D., K. Kim, Z. Li, & J. E. Bolander (2014). Flow field calculations within discrete models of multiphase materials. *Composites Part B: Engineering 58*, 293–302.

ASTM (2008). C 1585 04 Standard Test Method for Measurement of Rate of Absorption of Water by Hydraulic-Cement Concretes. Technical report, ASTM.

CEN (2002). EN 13057 Products and systems for the protection and repair of concrete structures - Test methods - Determination of resistance of capillary absorption. Technical report.

Esteves, L. P. (2011). Superabsorbent polymers: On their interaction with water and pore fluid. *Cement and Concrete Composites 33*(7), 717–724.

Grassl, P. & J. Bolander (2016). Three-dimensional network model for coupling of fracture and mass transport in quasi-brittle geomaterials. *Materials 9*(9), 1–18.

Hall, C. (1989). Water sorptivity of mortars and concretes: a review. *Magazine of concrete research 41*(147), 51–61.

Hall, C. & W. D. Hoff (2009). *Water Transport in Brick, Stone and Concrete* (2nd ed.), Volume 25. Spon Press.

Hong, G. & S. Choi (2017). Rapid self-sealing of cracks in cementitious materials incorporating superabsorbent polymers. *Construction and Building Materials 143*, 366–375.

Kim, J. S. & E. Schlangen (2010). Super Absorbent Polymers To Stimulate Self Healing in ECC. In *2nd International Symposium on Service Life Design for Infrastructure*, Number 1, pp. 849–858.

Lockington, D., J.-Y. Parlange, & P. Dux (1999). Sorptivity and the estimation of water penetration into unsaturated concrete. *Materials and Structures 32*(5), 342.

Luković, M., B. Šavija, E. Schlangen, G. Ye, & K. van Breugel (2016). A 3D lattice modelling study of drying shrinkage damage in concrete repair systems. *Materials 9*(7).

Pan, Y., A. Prado, R. Porras, O. Hafez, & J. Bolander (2017). Lattice Modeling of Early-Age Behavior of Structural Concrete. *Materials 10*(3), 231.

Qian, Z., E. Garboczi, G. Ye, & E. Schlangen (2016). Anm: a geometrical model for the composite structure of mortar and concrete using real-shape particles. *Materials and Structures 49*(1-2), 149–158.

Savija, B. (2014). *Experimental and Numerical Investigation of chloride ingress in cracked concrete*. Phd dissertation, TU Delft.

Šavija, B., J. Pacheco, & E. Schlangen (2013). Lattice modeling of chloride diffusion in sound and cracked concrete. *Cement and Concrete Composites 42*, 30–40.

Schlangen, E. & J. G. M. van Mier (1992). Experimental and Numerical Analysis of Micromechanisms of Fracture of Cement-Based Composites. *Cement & Concrete*

Composites (14), 105–118.

Snoeck, D. (2015). *Self-Healing and microstructure of cementitious materials with microfibres and superabsorbent polymers*. Phd dissertation, Ghent University.

Snoeck, D., S. Steuperaert, K. Van Tittelboom, P. Dubruel, & N. De Belie (2012). Visualization of water penetration in cementitious materials with superabsorbent polymers by means of neutron radiography. *Cement and Concrete Research 42*(8), 1113–1121.

Snoeck, D., L. F. Velasco, A. Mignon, S. Van Vlierberghe, P. Dubruel, P. Lodewyckx, & N. De Belie (2015). The effects of superabsorbent polymers on the microstructure of cementitious materials studied by means of sorption experiments. *Cement and Concrete Research 77*, 26–35.

Sweijen, T., C. van Duijn, & S. Hassanizadeh (2017). A model for diffusion of water into a swelling particle with a free boundary: Application to a super absorbent polymer particle. *Chemical Engineering Science 172*, 407–413.

Szymkiewicz, A. (2013). *Modelling Water Flow in Unsaturated Porous Media*, Volume 9.

Van Belleghem, B., R. Montoya, J. Dewanckele, N. Van Den Steen, I. De Graeve, J. Deconinck, V. Cnudde, K. Van Tittelboom, & N. De Belie (2016). Capillary water absorption in cracked and uncracked mortar - A comparison between experimental study and finite element analysis. *Construction and Building Materials 110*, 154–162.

Vervoort, S. (2006). *Behaviour of hydrogels swollen in polymer solutions under mechanical action*. Phd dissertation, Ecole Nationale Sup erieure des Mines de Paris.

Wang, L., J. Bao, & T. Ueda (2016). Prediction of mass transport in cracked-unsaturated concrete by mesoscale lattice. *Ocean Engineering 127*(August), 144–157.